*Nigerian Journal of Technology (NIJOTECH)*
*Vol. 45, No. 1, March 2026, pp. 75- 88*
*www.nijotech.com*

*Print ISSN: 0331-8443*
*Electronic ISSN: 2467-8821*
*https://dx.doi.org/10.4314/njt.v45i1.7*

# EXPERIMENTAL AND NUMERICAL ANALYSIS OF THE EFFECTS OF EXTRUSION REDUCTION RATIO AND LOAD ON AL 6063 FORMING PARAMETERS

**AUTHORS:**
*T. M. Azeez[1], H. S. Phuluwa[1], Z. J. Chihambakwe[1] and M. I. Adeoba[2]

**AFFILIATIONS:**
[1]Department of Industrial Engineering and Engineering Management, University of South Africa, Florida Campus, SOUTH AFRICA.
[2]Department of Mechanical, Bioresources and Biomedical Engineering, University of South Africa, Florida Campus, SOUTH AFRICA.

***CORRESPONDING AUTHOR:**
Email: azeeztm@unisa.ac.za

**ARTICLE HISTORY:**
**Received:** August 09, 2025.
**Revised:** January 10, 2026.
**Accepted:**January 22, 2026.
**Published:** April 29, 2026.

**KEYWORDS:**
*Extrusion parameter optimization, Extrusion ratio, Load, Model equation, Flow stress simulation*

**ARTICLE INCLUDES:**
Peer review

**DATA AVAILABILITY:**
On request from author(s)

**EDITORS:**
Chidozie Charles Nnaji

**FUNDING:**
None

## Abstract

*The applied load and extrusion reduction ratio effects on the Al 6063 alloy mechanical performance and microstructure were researched through a combined numerical and experimental approach. Extrusion trials were conducted at three loads and extrusion reduction ratios (20, 25, 30 MN) and (25 %, 50 %, 75 %) respectively. Tensile strength and Vickers hardness were measured, and quadratic second-order polynomial model was fitted for these responses' prediction. ANOVA confirmed that both parameters and their interaction are statistically significant ($p < 0.05$), and confirmatory experiments revealed model errors of less than 5 %. The peak hardness and tensile strength values of 88.25 HV and 280.15 MPa were obtained at 25 MN load and 12.5 % extrusion reduction ratio, while response-surface optimization revealed 48.32 % ratio and 27.44 MN load as the optimum for balanced strength and hardness. Extrusion process numerical simulations through QForm software were performed at the same extrusion reduction ratios and loads for material deformation and flow-stress evolution assessment. The simulations showed that flow stress increases with decreasing extrusion ratio, attaining its peak at 25 % ratio, and that higher loads reduce flow stress, enhancing fatigue resistance. The simulation time-displacement curves showed that a 25 % ratio requires the longest deformation time (≈108 min) compared with 12–24 min for 50–75 % ratios. Microstructural analysis affirmed grain refinement at 25 % and 50 % ratios, with the most uniform grain distribution.Both the numerical and experimental data simulations has shown that load and extrusion ratio optimization not only maximizes tensile strength and hardness but also influence flow stress and grain structure, enabling a detail framework for high-performance Al 6063 components production.*



## 1.0 INTRODUCTION

Aluminium (Al) is a lightweight, silvery white metal in the periodic table group 13 [1]. It is the most common nonferrous metal and the most prevalent metallic element in the Earth's crust [2]. Aluminium is commonly applicable in manufacturing and many other applications owing to its lightweight characteristics, abundance, and high strength-to-weight ratio. It has a density of 2.7 g/cm$^3$, and possesses excellent electrical conductivity and ductility, with almost two-thirds of the copper

***HOW TO CITE:***
Azeez, T. M., Phuluwa, H. S., Chihambakwe, Z. J. and Adeoba, M. I. "Experimental and Numerical Analysis of the Effects of Extrusion Reduction Ratio and Load on Al 6063 Forming Parameters", *Nigerian Journal of Technology*, 2026. 45(1), pp. 75 - 88. https://dx.doi.org/10.4314/njt.v45i1.7

conductivity [3]. However, it has lower electrical conductivity compared to copper, but its lower cost makes it a viable alternative. As a result, aluminium is commonly used in the production of high-voltage cables and wires, as well as in radio technology. Its ductility is next only to silver and gold, and it can easily be produced into aluminium foil thinner than 0.01 mm at temperatures ranging from 100 to 150 degrees Celsius [4]. Aluminium foils are commonly employed in the wrapping of cigarettes, candy, and other items. The strength of Aluminium increases at low temperatures without leading to brittleness, enabling it to be appropriate for applications like superconducting materials and cryogenic storage [5]. Due to its unique thermal conductivity, aluminium is appropriate for industrial applications like heat sinks and exchangers. In the production of complex-shaped aluminium products, the extrusion process is normally used[6].

Extrusion is a technique in which a material is plastically deformed by applying a force that causes the material to flow through a die opening [7]. The materials take on the die's cross-sectional shape, and if the material has acceptable characteristics, that shape is kept in the final extrudate [8]. Aluminium extrusion is a method that involves forcing aluminium alloy material through a die having a particular cross-sectional dimension. The aluminium is pushed through the die by a strong ram and exits from the die aperture. When it does, it is pushed out in a similar form to the die. Because of its forming ease and anodising reactivity, aluminium (Al 6063) is the most preferred type for aluminium extrusion. It also has a fantastic surface polish [9]. Aluminium extrusion is a reasonably straightforward technique to comprehend at a basic level. The force used is comparable to the force used when squeezing a tube of toothpaste with fingers. Squeezing causes the toothpaste to emerge from the tube's opening. The toothpaste tube's opening performs a similar job to an extrusion die [10]. The paste will come out as a long, solid extrusion because the orifice is a solid circle.

Extrusion process can be categorised based on either operation temperature or direction of ram movement [11]. The operating temperature category can further be subdivided into hot or cold extrusion. Hot extrusion of aluminium is carried out at a temperature above the recrystallisation temperature of aluminium but below its melting temperature[12]. The extrusion temperature of aluminium normally ranges between 350-550 ºC. In cold extrusion, the billet requires no pre-heating before extrusion. Ram movement direction category can also be subdivided into either direct extrusion or indirect extrusion. Direct extrusion occurs when the ram of the press forces the billet out of the die in a forward direction [13]. In this case, the final shape of the extruded product will take the shape of the die. In indirect extrusion, the hollow ram of the press was used in extrusion, and the billet flowed back to the hollow part of the ram. The final shape of the extruded product in this case will be the same as the hollow in the ram[13]. The following variables influence the extrusion procedure: extrusion ratio and speed, metal distortion resistance during extrusion, deformation, extrusion speed, friction conditions between billets and die contact surface, extrusion die angle, product section shape, billets length, and extrusion method [14].

The extrusion process is an important manufacturing method in complex-shaped aluminium products of high precision. However, extrusion procedures are mainly influenced by many forming variables, especially the extrusion ratio and the load, which are responsible for the microstructural properties of the products [15]. Despite the advantages of extrusion in the manufacturing of aluminium, there is a significant gap in comprehending the load and extrusion ratio effects on Al6063 during the extrusion process. This knowledge gap is responsible for the process optimisation challenges, leading to inconsistency and substandard products. In addressing this gap, the aim of the study is to investigate the load and extrusion ratio effects on the microstructure and mechanical properties of Al6063. Specifically, the study aims to investigate the extrusion ratio and load interaction on mechanical properties, and to optimise the extrusion process parameters to obtain an enhanced product with high quality. Through this, there will be contributions to the production of more efficient aluminium extrusion processes[16].

The current research gaps of insufficient comprehension between the extrusion ratio and load interactions, together with a lack of predictive ability in extrusion process simulation, needs to be tackled through numerical and experimental research findings of extrusion ratio and load as parameters in Al 6063 manufacturing, establishing a detailed understanding of their effects and material properties. Also, optimal extrusion parameter settings towards achieving the best product quality need to be established.


https://dx.doi.org/10.4314/njt.v45i1.7

## 2.0 MATERIALS AND METHODS

Aluminium 6063 grade (Figure 1) used for this research was obtained from the Engineering Material Development Institute (EMDI), Akure, Ondo State, Nigeria. The chemical composition of as as-received sample was analysed using a metal analysing spectrometer (HITACHI- OE750), concentrated on elements such as zinc, strontium, titanium, manganese, magnesium, chromium, silicon, copper and iron. The mild steel (AISI 1020) used for the development of the punch and die for the extrusion process was purchased at Owode Onirin, Lagos, Nigeria. The Nitric acid (Nital) that was selected as an etchant during microstructural assessment of the extruded aluminium product was purchased at a chemical store in Ojota, Lagos, Nigeria.

### 2.1 Preparation of Samples

The Aluminium 6063 sample (Figure 1a) was machined to a 58mm diameter (Figure 1b) using a lathe machine (FERVI 0497/250 – 0497). The die entrance channel had a diameter of 60mm. These dimensions were selected to allow proper die and billet (sample) fit for the extrusion process. Three dies of the same entry channel dimension (60mm) but different exit dimensions were fabricated. The exit dimensions of the dies are 15, 30 and 45mm, which are for 25 %, 50 % and 75 % extrusion ratios, respectively. These extrusion ratios imply the die exit to entry fractions.


**Figure 1**: Aluminium 6063 sample (a) prior machining for extrusion (b) after machining for extrusion

### 2.2 Response Surface Methodology

Response surface methodology was employed using Design Expert (version 12, Stat-Ease Inc.) to study the effect of extrusion ratio and load on tensile strength and hardness of extrudates. It entails the application of an analytical approach and effective modelling. This involves the use of design expert software to design the experiment as presented in Tables 1 and 2. There is an input variable and the responses to work with. In this case, the input variables are extrusion ratio and load, while the responses are tensile strength and hardness. The generated quadratic model is in the form presented in Equation. 1 [1]

where A = response; $\alpha_o$= total mean, $\alpha_m$ = linear effect of input factors $x_m$; $\alpha_{mn}$= linear by linear interaction effect; $\alpha_{mm}$ =quadratic effect of the input factor $x_m$ $\epsilon$ = random error term.

A mathematical model with various regression equations and second-order best fits was created. Multiple regression analysis was performed on each outcome using the provided equations. Analysis of variance (ANOVA) was used to analyse the model's significant terms for each output. The probability level that was judged to be less than 5% was used to evaluate the significance level. The model's suitability was assessed using $R^2$, adjusted $R^2$, predicted $R^2$, and prediction error sum of squares (PRESS). After fitting the models, residual analysis was performed to validate the ANOVA assumption. To accomplish fitting by the desirability function technique, polynomial maximisation and minimisation were used. The desirability, which ranges from 0 to 1, defines how closely it reaction approaches the ideal value [17]. Using the RSM response optimiser, optimal settings that yielded the best responses in terms of tensile strength and hardness were also determined


https://dx.doi.org/10.4314/njt.v45i1.7

### 2.3 Extrusion Process

The Aluminium 6063 samples, which have already been machined as presented in Figure 1b, were placed in an electric furnace, set at 550ºC for 30 minutes, and later transferred to the die, which has been lubricated with jatropha oil. In the experimental set up (Figure2a), the extruder was set to operate at a ram speed of 5mm/s. The whole set-up was coupled with a punch, and it was placed in an extruder for pressing. The three different loads set on the extruder for the extrusion process are 20 MN, 25 MN and 30 MN. Three dies with entry channel 60mm but different exit channel dimensions 15mm, 30mm, and 45mm were employed for the extrusion process. These corresponded to samples with extrusion ratios of 25 %, 50 %, and 75 % (Figure 2b), respectively. The measurement of the extrudates' tensile strength and hardness was determined with the use of a universal testing machine (Model No. UFc-14) and a Vickers hardness tester (Model No. 950-592). All the experiments were conducted thrice, and the average value represents the true results used for further analysis.

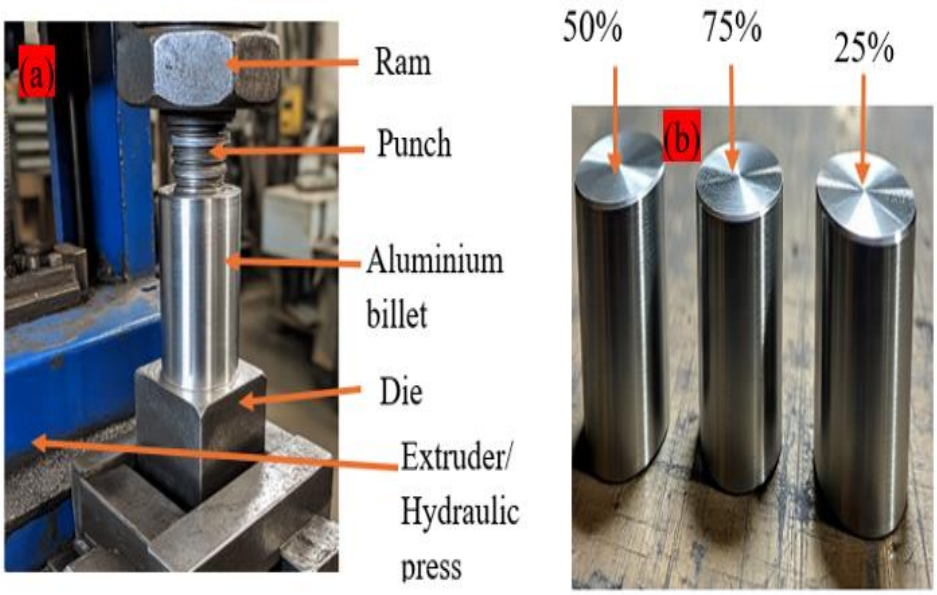


**Figure 2**: (a) Experimental extrusion setup showing the hydraulic ram, punch, and die assembly (b) extruded samples using three different die geometries

### 2.4 Experimental Design

Central Composite Design (CCD) of the Response Surface Methodology (RSM) was used for experimental design. All these are components of design expert software that are mainly used in the planning and optimisation of the experiment. The range of experimental details was presented in Table 1. 12 experimental runs were conducted in accordance with Table 2. From Table 1, the load range is between 20 to 30 MN while the extrusion ratio ranges between 25 % and 75 % and from Table 2, the midpoint value for load, which is represented as 0 on the code value, is 25 on the original value. Likewise, the midpoint value for extrusion ratio,

**Table 1**: Experimental design variables levels

| Factors | Code | -1 | +1 | -alpha | +alpha |
|---|---|---|---|---|---|
| **Load (MN)** | L | 20 | 30 | 17.93 | 32.07 |
| **Extrusion ratio (%)** | R | 25 | 75 | 12.5 | 87.5 |

which is also represented as 0 on the coded value, is 50 % on the true value. Please note that another two dies were developed for the extrusion ratio of 12.5 % and 87.5 %, which represent -α and +α in Table 2. The tensile strength and hardness test results of the extruded product after the extrusion process in conformance to Table 2 were used in the model generation for further response predictions. The


https://dx.doi.org/10.4314/njt.v45i1.7
http://creativecommons.org/licenses/by-nc-nd/4.0/

selection of extrusion ratio (25-75%) and load (20-30 MN) as extrusion parameters ranges is based on recommendations and choices from the existing research on the extrusion process [18].

**Table 2**: Experimental range design model

| S/N | CODED VALUE | | ORIGINAL VALUE | |
|---|---|---|---|---|
| | L | R | Load (MN) | Extrusion Ratio (%) |
| 1 | -1 | -1 | 20 | 25 |
| 2 | +1 | -1 | 30 | 25 |
| 3 | 0 | +1 | 25 | 75 |
| 4 | +1 | +1 | 30 | 75 |
| 5 | -α | 0 | 17.93 | 50 |
| 6 | +α | 0 | 32.07 | 50 |
| 7 | 0 | -α | 25 | 12.5 |
| 8 | 0 | +α | 25 | 87.5 |
| 9 | 0 | 0 | 25 | 50 |
| 10 | 0 | 0 | 25 | 50 |
| 11 | 0 | 0 | 25 | 50 |
| 12 | 0 | 0 | 25 | 50 |

## 2.5 Hardness Test

The hardness test was carried out using a 2000 kN accurate Vickers hardness testing machine (Model No. 950-592) following ASTM E18-22 Standard[17]. The extruded aluminium 6063 was machined to cuboidal shape, filled with a grinding machine and smoothened with emery paper to achieve a fine flat surface as presented in Figure 3. The prepared sample was then placed on the anvil of the hardness testing machine. A diamond indenter was rested on the sample for the 80 g preload application, which indicates the reference point that breaks through the surface for the surface finish effect reduction. This load was maintained constant for a dwell period of 12 seconds to enable an elastic recovery. The major load of 125 g was later removed, and the final indentation depth was measured and compared with the depth under preload of 80 g. The variation in indentation depth between the 80 g preload value and the final load of 125 g was evaluated. This variance was recorded as the hardness value. The procedures were repeated thrice per sample, and the mean value was used as the true value

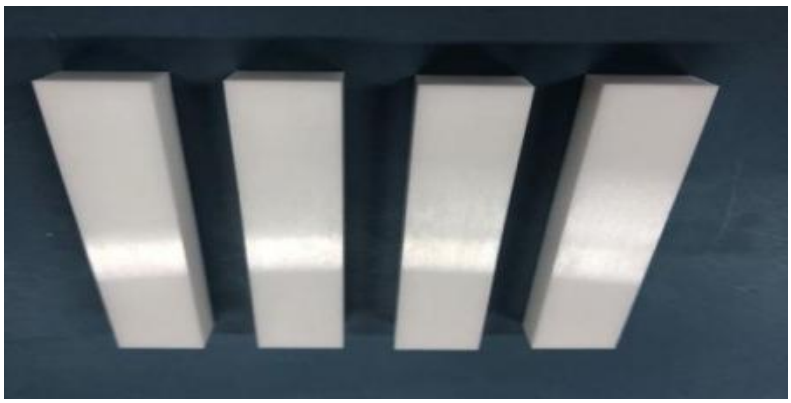

**Figure 3**: Machined specimen for hardness test

## 2.6 Tensile Test

This was evaluated using a 3000 kN blue star universal testing machine (Model No. UFc-14) following ASTM D638 protocol[17]. The extruded aluminium was first machined to a tensile test dimension, and samples are presented in Figure 4a and b. This dimension was chosen to match with configuration of the universal testing machine used. The procedure requires the mounting of the already machined test sample in the universal testing machine. The grip of the tensile tester held it firmly, and the pulling force of 55 kN was gradually introduced. The application of this force leads to the gradual extension of the specimen till necking occurs


https://dx.doi.org/10.4314/njt.v45i1.7
http://creativecommons.org/licenses/by-nc-nd/4.0/

and finally fractures. In the process, the gauge region extension, together with the applied force, was noted. The engineering strain and stress were derived through the measurement of elongation and the force, respectively

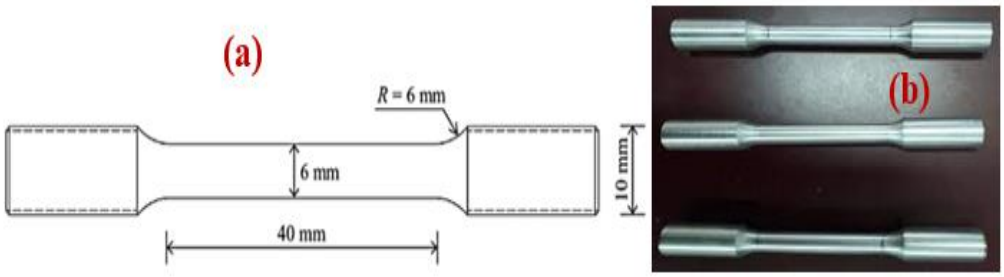


**Figure 4**: Tensile test (a) dimension (b) machined sample

### 2.7 Microstructural Analysis

Microstructural tests were conducted on both the unextruded sample and the samples extruded at different extrusion ratios to determine the grain refinement of the samples after extrusion. This involves the grinding of the sample surface with a grinding machine, followed by filling with emery papers of different grades. After all these, the samples were etched using Nital (Nitric acid) for the surface enabling in microstructural visualisation using an optical Microscope (Model: BS 2082).

### 2.8 Experimental Simulation

The simulation of the extrusion process was conducted using QForm Software (version 2.2), which is a finite element software dedicated to metal forming simulation. The stress flow of the extruded sample was examined through the simulation of the extrusion process at three different extrusion ratios 25%, 50 %, and 75 %. The aluminium was subjected to some assumptions like visco-plastic deformation, isotropy and homogeneity prior to deformation. However, aluminium alloys also have anisotropic flow tendency [19], which can reduce the assumption's accuracy. The extruder was supplied with a load of 20 MN and 30 MN to detect the simulated load effect on flow stress as well. The same configurations of the real experiment conducted earlier were imposed in the simulation. The billet (aluminium sample) was extruded at a temperature of 550 $^{o}$C and a ram speed of 5 mm/s

## 3.0 RESULTS AND DISCUSSIONS

### 3.1 Metal Analysis of Al 6063 Result

The mass metal analysis of the sample's composition is presented in Table 3. It was revealed through the result that magnesium (0.62 %) is a major alloying element. This is typical of Al 6063 grade [19]. Other major alloying element includes Silicon (0.45 %) and manganese (0.41 %). The minor alloying elements are Zinc (0.04 %), Strontium (0.05 %), Chromium (0.06 %), Copper (0.04 %) and Iron (0.35 %). The base element, which is aluminium, is 97.93%.

**Table 3**: Aluminium 6063 chemical composition

| Alloying Element | Zn | Sr | Ti | Mn | Mg | Cr | Si | Cu | Fe |
|---|---|---|---|---|---|---|---|---|---|
| **AA-6063 (%)** | 0.04 | 0.05 | 0.05 | 0.41 | 0.62 | 0.06 | 0.45 | 0.04 | 0.35 |

### 3.2 Response Results

The two responses in this study are tensile strength and hardness. As indicated in Table 4, for 13 runs of the experiments recommended by RSM, it was discovered that the maximum and minimum values of tensile strength are 280.15 MPa and 100.22 MPa, respectively. These values were obtained at experimental numbers 7 and 8 in Table 4, where there are the highest and lowest percentages of extrusion ratio. However, the two cases were extruded at a load of 25 MN. The hardness has shown a similar pattern of response when compared with tensile strength. The lowest extrusion ratio of 12.5 % gave the highest hardness of 88.25 HV, while the highest ratio of 87.5 % gave the lowest hardness of 31.57 HV. This may be because of a high compression rate, which leads to the breaking of larger grains into smaller ones and thereby makes the grain structure finer with increased hardness and tensile strength. The outcome that the lowest extrusion ratio of 12.5% led to the highest tensile strength, which complies with the finding of Zheng


https://dx.doi.org/10.4314/njt.v45i1.7
http://creativecommons.org/licenses/by-nc-nd/4.0/

et.al (2020), who presented a similar report in their research on aluminium extrusion [7]. Also, this outcome is substantiated by the Hall-Petch formulation that forecasts that small grains from smaller extrusion ratios can lead to higher strength [20]. This implies that lower extrusion ratios may be advantageous in high-strength applications. This could be connected to the reduced strain hardening effect at lower extrusion ratios, which enables more consistent microstructure and enhanced mechanical characteristics.

Application areas of this research include the high-strength aluminium components production for the automotive and aerospace industries.

**Table 4**: Inputs and response variables of extrusion

| No | Input | | Responses | |
|---|---|---|---|---|
| | **Load (MN)** | **Extrusion ratio (%)** | **TS (MPa)** | **Hardness (Hv)** |
| **1** | 20 | 25 | 205.54 | 64.75 |
| **2** | 30 | 25 | 223.63 | 70.44 |
| **3** | 25 | 75 | 115.24 | 36.30 |
| **4** | 30 | 75 | 140.55 | 44.27 |
| **5** | 17.93 | 50 | 153.62 | 48.39 |
| **6** | 32.07 | 50 | 190.55 | 60.02 |
| **7** | 25 | 12.5 | 280.15 | 88.25 |
| **8** | 25 | 87.5 | 100.22 | 31.57 |
| **9** | 25 | 50 | 170.43 | 53.69 |
| **10** | 25 | 50 | 169.88 | 53.51 |
| **11** | 25 | 50 | 171.23 | 53.94 |
| **12** | 25 | 50 | 170.31 | 53.65 |
| **13** | 25 | 50 | 170.31 | 53.65 |

### 3.3 Statistical Analysis and Model Development

A second-order polynomial model in quadratic form was used in forecasting the responses for a given range of extrusion factors considered (extrusion ratio and load). This was generated from the RSM of the Design Expert application. Therefore, the two responses were predicted by Equations. 2 and 3.

$$X = 170.43 + 11.95A - 53.48B + 1.81AB - 1.65A^2 + 7.40B^2. \quad (2)$$

$$Y = 53.69 + 3.76A - 16.85B + 0.57AB - 0.5209A^2 + 2.33B^2 \quad (3)$$

Where X is the value for tensile strength,
Y is the value for hardness,
A is the load in MN,
B is the extrusion ratio in percentage.

**Table 5**: Variance analysis for the hardness and tensile strength models

| Source | Tensile Strength | | Hardness | |
|---|---|---|---|---|
| | F Value | p- value | F Value | p-value |
| **Model** | 33.31 | < 0.0001 | 33.31 | < 0.0001 |
| A-load | 7.78 | 0.0269 | 7.77 | 0.0270 |
| B-Ratio | 155.76 | < 0.0001 | 155.78 | < 0.0001 |
| AB | 0.0887 | 0.0745 | 0.0892 | 0.0739 |
| $A^2$ | 0.1285 | 0.0306 | 0.1295 | 0.0296 |
| $B^2$ | 2.60 | 0.0512 | 2.59 | 0.0513 |

In determining the model suitability for the prediction of the stated responses, Analysis of Variance (ANOVA) was employed, and this is displayed in Table 5. The model is said to be significant at P-value < 0.05 [21]. In this case, extrusion ratio and load are significant model terms because they both have P-values of <0.0001 and 0.0268. However, before a model can be declared insignificant, the P-value should be greater than 0.1000. Therefore, the interaction between extrusion


https://dx.doi.org/10.4314/njt.v45i1.7
http://creativecommons.org/licenses/by-nc-nd/4.0/

load and ratio (AB), load$^2$($A^2$) and the ratio$^2$ ($B^2$) with the P-values, 0.0745, 0.0306 and 0.0512, respectively, are also significant, but their significance levels are smaller compared to ordinary load (A) and extrusion ratio (B). Extrusion ratio has the highest level of significance, and this is revealed in Figure 5a and b in both tensile strength and hardness, respectively. In the analysis of the second-order model fitting presented in Table 6, the model can be described as a perfect fit for prediction because the coefficient of correlation ($R^2$) is greater than 95% for both tensile strength and hardness (95.97% for both cases). Another sign of strong model fit is a variance of less than 0.2 between predicted and adjusted $R^2$ [1]. In this situation, the difference is zero.

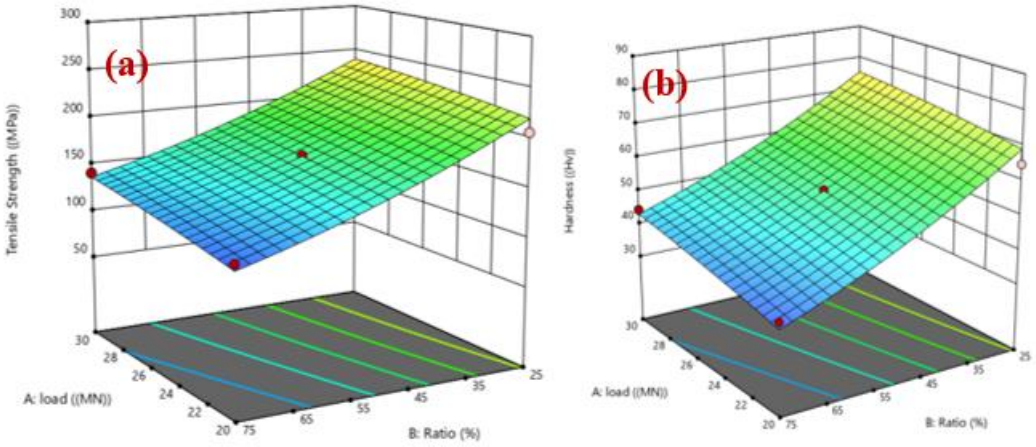


**Figure 5**: 3D response plot of extrusion ratio and load to (a) tensile strength (b) hardness

**Table 6**: ANOVA results from second order model fitting

| Model summary characteristics | Tensile Strength | Hardness |
|---|---|---|
| Standard Deviation | 12.12 | 3.82 |
| $R^2$ | 0.9597 | 0.9597 |
| Adjusted $R^2$ | 0.9309 | 0.9309 |
| Predicted $R^2$ | 0.9134 | 0.9134 |
| Adeq Precision | 18.4505 | 18.4521 |

Furthermore, appropriate precision in measuring signal-to-noise ratio should be better than 4. Tensile strength is 18.4501, and hardness is 18.452. The model validation was done through numerical predictions in comparison with experimental outcomes. Tensile strength is revealed in Figure 6a, while hardness response is presented Figure 6b. In both cases, the numerical values closely align with the experimental pattern across the three applied loads (20 MN, 25 MN, 30 MN) and reduction percentage (25 %, 50 %, 75 %). The tensile strength average deviation between measured and predicted value was <5 %, and <4 % for hardness, implying good agreement. Error bars on the experimental data represent standard deviations from three repeated tests, and the numerical predictions fall within these ranges for most conditions, confirming the model's reliability.

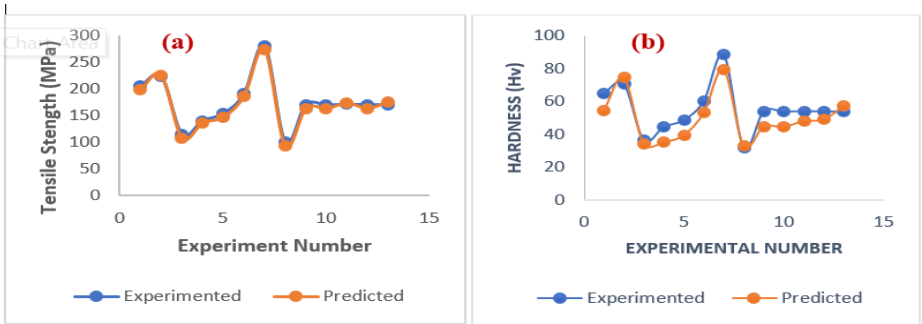


**Figure 6**: Plot of comparison between experimented and predicted (a) tensile


https://dx.doi.org/10.4314/njt.v45i1.7
http://creativecommons.org/licenses/by-nc-nd/4.0/

strength response (b) hardness response

### 3.4 Confirmation Experiments

Based on the recommendation of RSM, the most favourable (optimum) value of these two selected process variables, i.e., extrusion ratio and load, is 48.317 % and 27.244 MN, respectively. This will produce aluminium with 179.044 MPa tensile strength and 56.40 HV hardness. Further details of this are illustrated in the optimisation ramp presented in Figure 7. To validate these predictions, a confirmatory experiment was conducted and narrated in Table 7. Percentage variations between the conducted experiment and the model prediction for both tensile strength and hardness were also presented in the same Table 7. The variation percentages for the 3 experimental trials are 4.73 %, 4.66 % and 3.71 % for tensile strength, while hardness percentage variations are 4.33 %, 4.24 % and 3.37 %

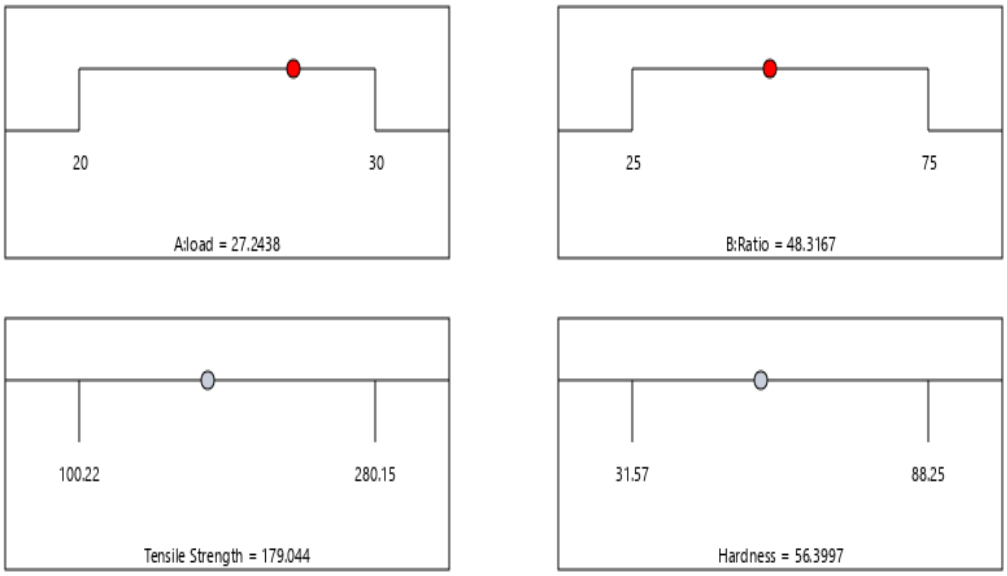


**Figure 7**: Process ramp for optimization

**Table 7**: Confirmation experiment results for tensile strength and hardness of AA 6063 alloy

| Trials | Tensile strength (MPa) | | Hardness (Hv) | | % Variation | |
|---|---|---|---|---|---|---|
| | Experimental response | Model prediction | Experimental Response | Model Prediction | Tensile strength | Hardness |
| 1 | 187.402 | 179.044 | 54.01 | 56.40 | 4.66 | 4.24 |
| 2 | 186.05 | 179.044 | 54.50 | 56.40 | 3.91 | 3.37 |
| 3 | 187.51 | 179.044 | 53.96 | 56.40 | 4.73 | 4.33 |

### 3.5 Load and Extrusion Ratio Simulation Result

Figure 8a shows the simulation of the flow stress distributions of the unextruded aluminium sample. The flow stress level falls between 128 MPa and 164.3 MPa for the minimum and maximum levels, respectively. The stress flow also looks uniform within this range because it has not undergone plastic deformation. Figure 8 b-d are the flow stress distributions of the samples extruded at a 25 % ratio, 50 % ratio and 75 % ratio. The flow stress is the measure of resistance to deformation. This implies that an increase in flow stress in the material will lead to a higher fatigue failure rate. Therefore, the drop in minimum/maximum flow stress from 128 MPa/ 164.3 MPa in Figure 8a to 28.52 MPa/112.6 MPa, 25.2 MPa/57.45 MPa and 32.42 MPa /54.1 in Figure 8b, c and d, respectively, can be associated with the plastic deformation the materials have experienced after the extrusion. A significant drop in maximum/minimum flow stresses was noticed between Figure 8a and b (unextruded and 25% extrusion ratio). It dropped from 128 MPa/ 164.3 MPa to 28.52 MPa/112.6 MPa. Also, the dropping of flow stress was significant between Figure. 8b and c (25% and 50% extrusion ratio) because it dropped from 25.82MPa/112.6 MPa to 25.32MPa/ 57.45 MPa. The dropping rate in flow stress between


https://dx.doi.org/10.4314/njt.v45i1.7

Figure 8c and is very low compared to the other two phases. It dropped from 25.32/57.45 MPa to 32.42/54.1 MPa. In other words, the flow stress decreases with an increase in extrusion ratio. This is because as the extrusion ratio R value increases, so does the required force for extrusion, as well as the pressure of the developed material on the tools. As a result, the increase in force and flow rate not only raises the load on the die but also substantially enhances the flow stress [22].

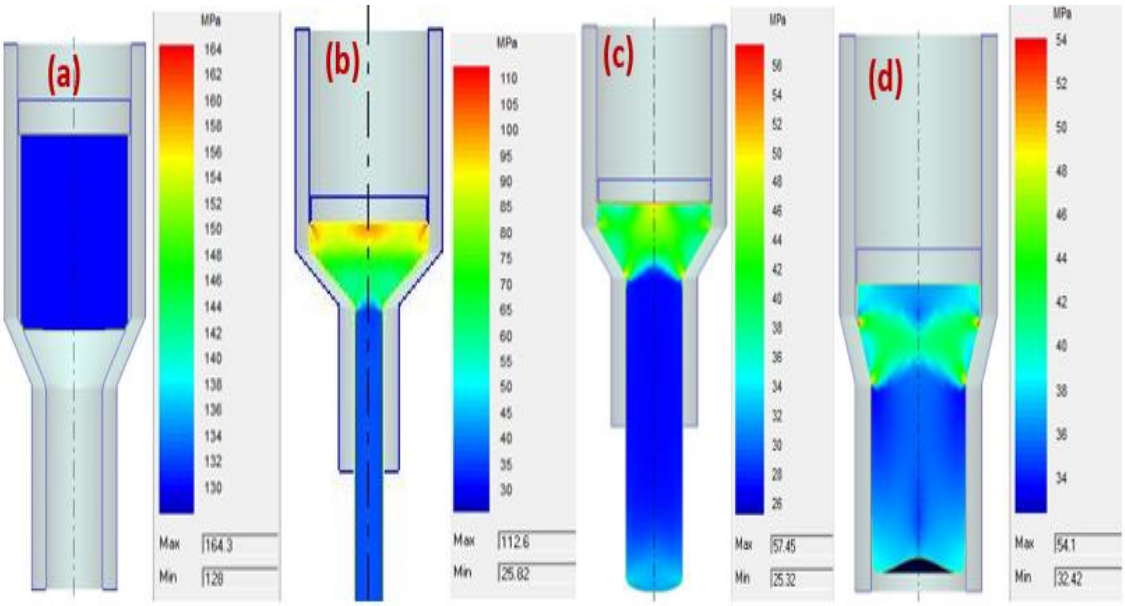


**Figure 8**: Flow stress distributions in (a) unextruded billet, (b) extruded at 25 % ratio, (c) 50 % ratio, and (d) 75 % ratio

Similarly, load also has an impact on flow stress distributions. As indicated in Figure 9a and b, flow stress decreases with an increase in extrusion load. Using a constant extrusion ratio of 50% but changing the extrusion load from 20 MN to 30 MN led to a decrease in the minimum/maximum flow stress from 162 MPa/55.78 MPa to 117.6 MPa/ 35.11 MPa. This is because, in the extrusion of materials, when high loads are used, less flow stress will be induced and consequently make the material fatigue resistant [6]

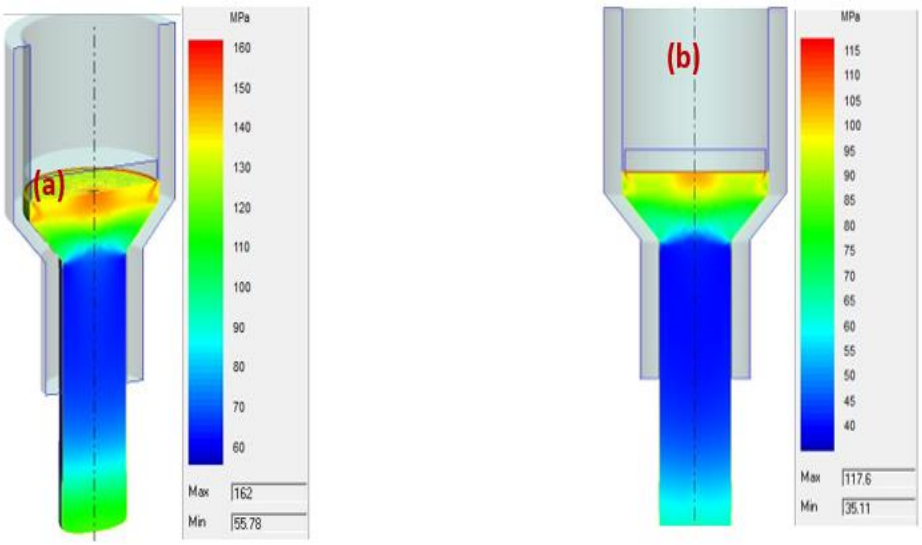


**Figure 9**: Flow stress distribution of the sample extruded at (a) 20 MN, (b) 30 MN

The time displacement graph for all aluminium samples extruded at different ratios specified was uploaded from the simulation data and presented in Figure 10. It was discovered that the aluminium sample extruded at a 25 % ratio took the longest time for aluminium to deform. It took 1.8 hours (108


https://dx.doi.org/10.4314/njt.v45i1.7
http://creativecommons.org/licenses/by-nc-nd/4.0/

minutes) for aluminium subjected to extrusion under this ratio to deform. The sample extruded at 50 % and 75 % ratio requires 0.2 hours (12 minutes) and 0.4 hours (24 minutes) respectively to deform completely. The large variance in time taken for materials to deform in a 25 % ratio compared to other ratios experimented may be responsible for the large flow stress gap at the same phase presented in Figure 8. This is due to the 25 to 30 % friction decrease, which enables the extrusion of thicker billets, faster speeds, and the capacity to extrude thinner cross-sections [23] [24].

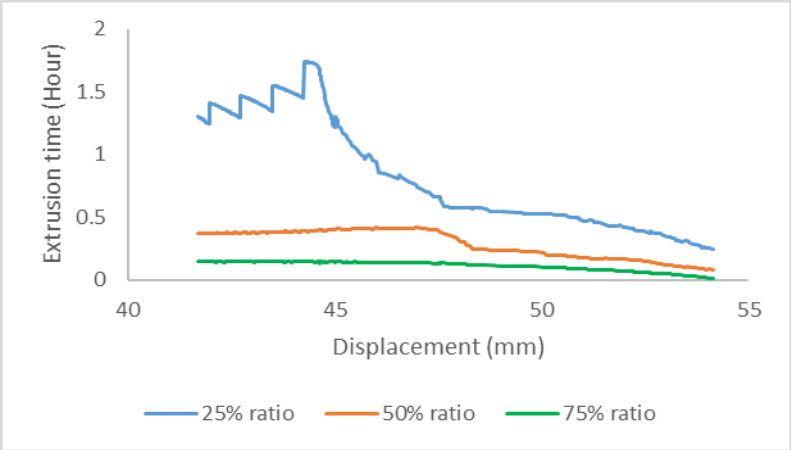


**Figure 10**: Time displacement graph for aluminium extruded at different ratios

### 3.6 Grain Refinement at Different Extrusion Ratios Using Optical Microscope

The outcomes of the grain refinement are shown in Figure 11, revealing the extruded and as-received samples' microstructure at different extrusion ratios. The Accurate BS2082 optical microscope with 1000x magnification was used for the microstructural. The grain size assessment was carried out using the linear intercept technique, as narrated in ASTM E112[17]. The extruded samples were ground and polished to a mirror finish and later etched using Nital (Nitric acid) to show the grain boundaries. The measurement of average grain size was evaluated through multiple measurements obtained from various sections of the samples. Figure 11a presents the grain size of as as-received (unextruded) sample, which is very coarse with a larger particle size. Grain size reduction with finer particles was noticed in Figure 11b contrast to Figure 11a. This is due to the extrusion at a 75 % Ratio.

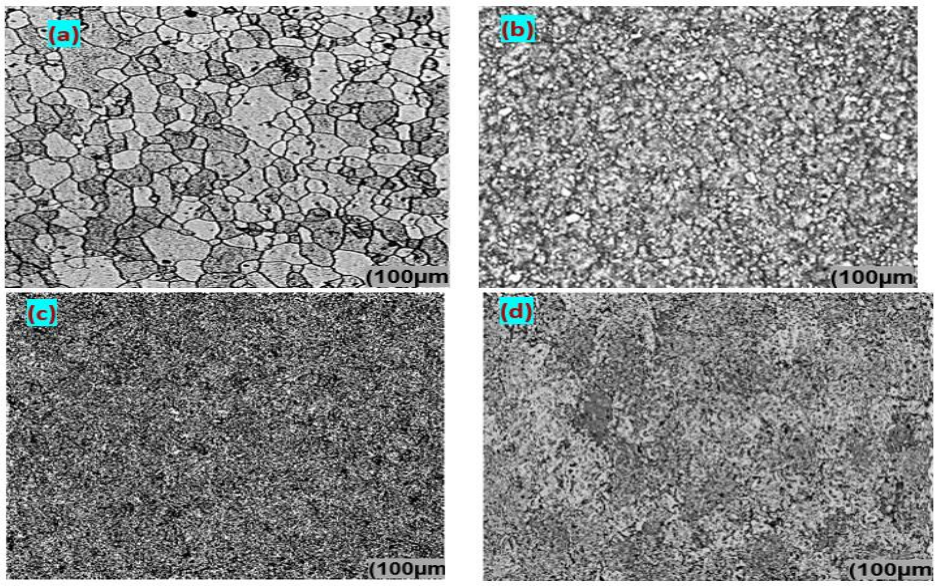


**Figure 11**: Grain refinements of the samples extruded at (a) As received sample, (b) 75 % extrusion ratio, (c) 50 % extrusion ratio, (d) 25 % extrusion ratio, Mag X 1000


https://dx.doi.org/10.4314/njt.v45i1.7

Further grain refinement with uniform structure was noticed after the extrusion at a 50 % ratio, as presented in Figure 11c. Finer particles were also revealed in Figure 11d after the extrusion at 25 %. However, the grain particles in Figure 11d (25 % ratio) are not uniformly distributed compared to Figure 11c. In general, a reduction in extrusion ratio can significantly enhance the grain structures of the extruded products. In all the samples, extrusion at a 50 % ratio yielded the best grain structure, finest and uniform particles of all the extrusion ratios considered in this research. This result conforms with the model developed, which identified an extrusion at a 48.316 ratio as the optimum value of this process. Also, because of huge grain dislocation that normally occurs under high reduction ratio, finer and tougher new material emerges compared to that extruded under low reduction ratio [25] [26][27].

## 4.0 CONCLUSION

The research has resulted in strong connection and most pronounced relationship between mechanical characteristics and grain size with extrusion parameters. Most important was that the increase in tensile strength and hardness was influenced by the decrease in extrusion ratio with resulted decrease in microstructure, while the lowest extrusion ratio led to the attainment of the highest tensile strength of 280.15 MPa with finer grain size. Furthermore, a 50% extrusion ratio was found to produce the finest and regular grain size with the optimal and average mechanical properties. More findings showed that reduction in extrusion ratio increases hardness and tensile strength of the extrudates, the flow stress was found to increase with decreasing extrusion ratio, the extrusion ratio was found to increase with decreasing extrusion process time, the extrusion load was found to increase with decreasing flow stress, and the finest and most uniformgrain size was visualised at a 50 % extrusion ratio at higher optimal mechanical characteristics. These research outcomes have substantially impacted the aluminium extrusion processes in industries that require wear resistance and high strength for operation.

## REFERENCES


[1] Azeez, T. M. Mudashiru, Asafa, T. B. Adeleke, A. A. Yusuf, A. S. and Ikubanni P.P., "Mechanical Properties and Stress Distribution in Aluminium 6063 Extrudates Processed by Equal Channel Angular Extrusion Technique," *Australlian Journal of Mechanical Engineering*, 14(53), pp. 1–9, 2021. https://doi.org/10.4028/p-Jjia46

[2] Mustapha, H. Mohamed, B. and Rabia, K., "Reliability approach, for lifetime prediction of the aluminium extrusion dies", *Research on Engineering Structures & Materials,* 11(1): pp 59-71, 2025.

[3] Arty, A. B. Ze'ev, S. B. and Frage, N., "Teaching metal- forming process using a laboratory micro-extrusion press," *Minerals, Metals and Materials series*, 3(4), pp. 55–67, 2020. doi: http://doi.org/10.1007/978-3-030-36556-1.

[4] Atur, K. and Mayank, M. "Optimization of process parameters in extrusion of aluminium", *International Journal of Science, Engineering, and Technology,* 10(4) pp 1-4, 2022. https://www.ijset.in/wp-content/uploads/IJSET_V10_issue4_271.pdf

[5] Kamala, N. S. and Vijayaraghavan, K., "Green Synthesis of Silver and Gold Nanoparticles Using Aloe Vera Gel and Determining its Antimicrobial Properties on Nanoparticle Impregnated Cotton Fabric," *Journal of Nanotechnology Research*, 2(3), pp. 42–50, 2020. https://www.doi.org/10.26502/jnr.2688-85210015

[6] Daramola, O. Ogunsanya, O. Akintayo, O. Oladele, I. Adewuyi, B. and Sadiku, E., "Mechanical properties of Al 6063 metal matrix composites reinforced with agro-waste silica particles," *Leanardo Electronic Journal of Practices and Technology*, 19(33), pp. 89–104, 2019.

[7] Zheng, J. Y. Shi, S. Q. and Fu, M. W., "Progressive microforming of pin-shaped plunger parts and the grain size effect on its forming quality," *Materials and Designs*, 187, pp. 1-13, 2019. doi: 10.1016/j.matdes.2019.108386.

[8] Marco, N. Lorenzo, D. and Adrian, H.A., "Smart extrusion via data-driven prediction of grain size and peripheral coarse grain defect formation", *Scientific*

*Reports,*15(9518), pp. 1-19, 2025. https://doi.org/10.1038/s41598-025-94884-4

[9] Marco, N. Riccardo, P. Sara, D. Barbara, R. Lorenzo, D. and Adrian, H.A., "Microstructure prediction using finite element simulation and artificial neural network for extrusion of AA6XXX aluminium alloy", *Material Research Forum*, 54, pp 764-771, 2025. https://doi.org/10.21741/9781644903599-82

[10] Li, W. T. Li, H. and Fu, M. W., "Interactive effect of stress state and grain size on fracture behaviours of copper in micro-scaled plastic deformation," *International Journal of Plasticity*, 114, pp. 126-143, 2019. doi: 10.1016/j.ijplas.2018.10.013.

[11] Zihui, W. Zhixin, Z. Qianyu, X. Yanjun, Z. Qiang, Q. Xuyang, L. Weiping, H. Quingchun M. and Hua, L., "Fatigue life estimation of open-hole cold-extrusion strengthened structures using continuum damage mechanics and optimized machine learning models" *Engineering Fracture Mechanics,* 318(7), 110915, 2025. https://doi.org/10.1016/j.engfracmech.2025.110915

[12] Wang, C., "Size effect affected mechanical properties and formability in micro plane strain deformation process of pure nickel," *Journal of Materials Processing Technology*, 258, 2018. doi: 10.1016/j.jmatprotec.2018.04.001.

[13] Yalçinkaya, T. Demirci, A. Simonovski, I. and Özdemir, I., "Micromechanical Modelling of Size Effects in Microforming," *Procedia Engineering*, 207, pp. 997-1003. 2017. doi: 10.1016/j.proeng.2017.10.865.

[14] Azeez, T. M. Mudashiru, L. O. Adeleke, A. A. and Adeshina, O. A., "Effect of Heat Treatment on Micro-Hardness and Micro-structural Properties of Al-6063 Alloy Reinforced with Silver Nanoparticles (AgPNs)," *International Conference on Engineering for Sustainable World* 1107(1), pp. 1–8., 2021. https://doi.org/10.1088/1757-899X/1107/1/012013?urlappend=%3Futm_source%3Dresearchgate.net%26utm_medium%3Darticle

[15] Alejandro, F. Pablo, Z. David, B. Fernado, P. and Pedro, F., "Evaluating the influence of machine type on surface roughness in material extrusion", *International Journal of Advanced Manufacturing Technology*, 8, pp 54-60, 2025. https://doi.org/10.1007/s00170-025-15595-8.

[16] Mohammed, I. U. and Senthil, K. S., "Application of response surface methodology in optimizing process parameters of twist extrusion process for aluminum aa 6061- T6 alloy," *Measurement*, 94, pp. 126-138., 2016. doi: 10.1016/j.measurement.2016.07.085

[17] "ASTM International. Standard Test Methods for Tension Testing of Metallic Materials. ASTM E8/E8M. West Conshohocken, PA, USA. 2018.

[18] Zi-Ning, L. Xiao-Qing, T. Dingyifei, M. Shahid, H. Lian, X. and Jiang, H., "Optimization of extrusion-based silicone additive manufacturing process parameters based on improved kernel extreme learning machine", *Chinese Journal of Polymer Science*, 43, 5, pp 848-862, 2025. https://doi.org/10.1007/s10118-025-3306-x

[19] Martins, H. Patricia, V. Millan, F. and Stepan, K. " The effects of strain rate and anisotropy on the formability and mechanical behaviour of aluminium alloy 2024-T3", *Metals,* 41(1), pp98-106, 2024. https://doi.org/10.3390/met14010098

[20] Jose, C. R. Miguel, P. Pablo, N. Carola, M. Gilberto, S. Humberto, P. Juan, F.V. and Ameet. K.A., "Effect of processing parameters on printability and mechano-biological properties of polycaprolactone-bioactive glass composites for 3D printed scaffold fabrication", *Polymers,*17, 11, 1554, 2025. https://www.mdpi.com/2073-4360/17/11/1554#

[21] Krzysztof, F. and Marcin, B., "Use of response surface methodology in

characterization of properties of recycled high-density polyethylene/ground, tire rubber," *Polymery*, 59(6), pp. 488–494, 2014.https://doi.org/10.14314/polimery.2

on size effect in microtensile deformation of a nickel-based superalloy," *Materials Science and Engineering: A*, 766(138405), pp. 1-10. 2019. https://doi.org/10.1016/j.msea.2019.138405

[23] Hu, J. Shimizu, T. Yoshino, T. Shiratori, T. and Yang, M., "Evolution of acoustic softening effect on ultrasonic-assisted micro/meso-compression behavior and microstructure", *Ultrasonics*, 107(106107), pp. 15-22, 2020. doi: 10.1016/j.ultras.2020.106107.

[24] Ogbonnaya, M. Ojolo, S.J. Oyefule, O. and Abudu, M., "Design and fabrication of a waste plastic filament extruder," *Nigerian Journal of Technology,* vol. 43 (3), pp. 602-609, 2024. https://doi.org/10.4314/njt.v43i3.2

[25] Yu M. W., Li Z. M., and Zhang Y. F., "Study of microstructural grain and geometric size effects on plastic

014.488

[22] Zhu, Q. Cheng, L. Wang, C. Chen, G. Qin, H. and Zhang, P., "Effect of δ phase

heterogeneities at grain-level by using crystal plasticity modeling with high-fidelity representative microstructures,"*International Journal of Plasticity*, 100, 4, 69-89, 2018. https://doi.org/10.1016/j.ijplas.2017.09.011.

[26] Azeez, T.M. and Phuluwa, H. S., "A multi-faceted investigative approach to ram speed, extrusion temperature and die exit width effects on mechanical properties of extruded al 6063 alloy," *Engineering Solid Mechanics*, 13(4), pp. 363–372, 2025. doi: 10.5267/j.esm.2025.8.002

[27] Francy, K.A. and Rao, C.S., "Multi response optimisation of cold extrusion parameters on AA 2024 alloy using TOPSIS," *Journal of the Institution of Engineers*, 106(2) pp. 1061–1075, 2025. https://link.springer.com/article/10.1007/s40033-024-00700-0